Clays and Clay Minerals, Vol. 45, No. 6, 789–802, 1997.

MIGRATION OF CATIONS IN COPPER(II)-EXCHANGED MONTMORILLONITE AND LAPONITE UPON HEATING

C. MOSSER,[1] L. J. MICHOT,[2] F. VILLIERAS[2] AND M. ROMEO[3]

[1] Centre de Géochimie de la Surface, UPR 6251 du CNRS, 1, rue Blessig 67084 Strasbourg Cedex, France

[2] Laboratoire "Environment et Minéralurgie", INPL-ENSG et URA 235 du CNRS, B.P. 40, 54501 Vandoeuvre Cedex, France

[3] Institut de Physique et Chimie des Matériaux, UMR 46 du CNRS, 23, rue du Loess, 67037 Strasbourg Cedex, France

Abstract—Two clay minerals, a dioctahedral, Na-montmorillonite from Wyoming and a trioctahedral, synthetic Na-laponite, were exchanged by cupric (Cu(II)) ions and subsequently heated at 100 °C intervals up to 500 °C. The resulting materials were analyzed by chemical analysis, X-ray diffraction (XRD), cation exchange capacity (CEC) measurements, combined thermogravimetric and differential thermal analysis (TGA-DTA), infrared (IR) spectroscopy, electron paramagnetic resonance (EPR) and X-ray photoelectron spectroscopy (XPS). Montmorillonite exhibits a well-known Hoffmann–Klemen effect in that, when heated, cupric (Cu) ions migrate into the lacunae of the octahedral sheet, where they compensate the negative charge deficit of the clay layer. In the case of laponite, CEC measurements and spectroscopic measurements reveal that Cu ions migrate into the octahedral sheet where they replace Li and Mg ions. After heating at 200 °C, approximately half the interlayer Cu ions are exchanged. The exchange appears to be 1 Cu for 1 Li, resulting in a slight decrease of the negative charge of the layer. After heating at 300 °C, the remaining Cu ions are exchanged by either 1 Mg or 2 Li, which does not result in any further charge reduction. At 400 °C, some of the extracted Mg remigrates into the structure and exchanges some Li (1 Mg for 2 Li). The final product at 400 or 500 °C is then a Li-laponite with Cu(II) in the octahedral sheet.

Key Words—CEC Measurements, Cu-Laponite, Cu-Montmorillonite, EPR, Hofmann–Klemen Effect, IR, XPS.

INTRODUCTION

Upon heating of dioctahedral smectites with octahedral charge deficit around 200–300 °C, small interlayer cations leave their interlamellar position to migrate into the structure. This corresponds to the well-known Hofmann–Klemen effect (Hofmann and Klemen 1950), which is the basis of the Greene–Kelly test (Greene–Kelly 1953, 1955) used to differentiate montmorillonite from beidellite. There is still much debate about the precise location of these cations after their migration: 1) migration of interlayer cations into vacant octahedral sites and 2) migration of interlayer cations into the bottom of the hexagonal cavities of the tetrahedral layer (Calvet and Prost 1971; McBride and Mortland 1974; Brindley and Lemaitre 1987; Alvero et al. 1994; Heller-Kallai and Mosser 1995).

In the present study, we compared a dioctahedral mineral, montmorillonite, with a trioctahedral one, laponite. Because of its structure, after heating, interlayer cations of laponite should not migrate any further than the bottom of the hexagonal cavity; whereas, for montmorillonite, the cations could migrate towards the octahedral vacancies. We chose to study the migration of Cu(II) because Cu ions are excellent probes, as their local environments can be monitored accurately by EPR spectroscopy and should allow distinguishing between the 2 types of sites.

Both minerals were Cu-exchanged and heated subsequently to 500 °C in steps of 100 °C. The samples were then studied by XRD, CEC measurements, thermal analysis and diffuse reflectance IR, XPS and EPR spectroscopy.

MATERIALS

Two different clay minerals were used in this study. Laponite is a synthetic hectorite sample provided by Laporte Adsorbents (Widnes, Cheshire, United Kingdom). Its structural formula determined from chemical analyses is $Si_8(Mg_{5.45}Li_{0.55})O_{20}(OH)_4Na_{0.55}$ and the sample contains approximately 1% of sodium carbonate (Na_2CO_3) (Cases et al. 1981). Wyoming montmorillonite (sample SWy-1) was obtained from the Clay Minerals Source Repository, University of Missouri. It was purified before use by sedimentation in order to eliminate coarse fractions (quartz and carbonates) and exchanged 3 times in NaCl 1 *M* to ensure homoionicity. After purification and washing in water, chemical analyses yielded the following structural formula, which can be written as $(Si_{7.96}Al_{0.04})(Al_{3.12}Mg_{0.45}Fe^{II}_{0.16}Fe^{III}_{0.27})O_{20}(OH)_4Na_{0.65}$. The starting laponite will be referred to as "Lap-Na" and the starting montmorillonite as "Mont-Na".

Both clays were Cu-exchanged using the following procedure: 40 g of clay was dispersed in 1 L of 0.5 *M* copper sulfate. The exchange procedure was carried out 3 times. After exchange the clays were washed 7 times in demineralized water, and the final suspensions

Table 1. The $d(001)$ values of montmorillonite and laponite after Cu exchange and subsequent heat treatment.

Sample	Heating temperature (°C)	$d(001)$ (Å)
Lap-Na	25	11.3
Lap-Cu	25	10.6
Lap-Cu	100	11.3
Lap-Cu	200	10.6
Lap-Cu	300	10.6
Lap-Cu	400	10.9
Lap-Cu	500	10.6
Mont-Na	25	12.6
Mont-Cu	25	12.3
Mont-Cu	100	12.4
Mont-Cu	200	9.9
Mont-Cu	300	9.8
Mont-Cu	400	9.6
Mont-Cu	500	9.5

were freeze-dried. The 2 samples obtained will be referred to as "Lap-Cu" and "Mont-Cu".

Then 1.5 g samples of Lap-Cu or Mont-Cu were heated in a programmable oven at 100, 200, 300, 400 and 500 °C. The temperature ramp was always 1 °C/min and the final temperatures were maintained for 6 h. In the case of Mont-Cu, 1 additional sample was maintained at 500 °C for 24 h.

METHODS

Chemical Analyses

Chemical analyses of the samples were performed at the Centre de Recherches Pétrographiques et Géochimiques (CRPG) in Vandoeuvre les Nancy, France, by inductively coupled plasma (ICP) measurements on a Jobin Yvon 70 quantometer.

CEC Measurements

The CECs of all samples were determined by exchanging the cations with the cobaltihexamine ion $[Co(NH_3)_6]^{3+}$ (Rémy and Orsini 1976). Clay samples of 400 mg were dispersed in 40 mL of a 0.05 *M* cobaltihexamine solution. The suspension was stirred for 2 h and centrifuged twice. The equilibrium concentration of the supernatant in cobaltihexamine was determined colorimetrically (Co absorption band at 473 nm) on a UV-visible spectrometer (Simadzu UV 2100) that yields the CEC. Concurrently, the supernatant was analyzed by atomic absorption to determine the kind and quantity of the exchanged cations.

XRD

X-ray diffraction patterns were obtained on powdered freeze-dried samples at CRPG. The apparatus used was a Jobin Yvon Sigma 2080 diffractometer with Cu$K\alpha_1$ radiation.

Thermal Analyses

A Ugine–Eyraud B70 balance (Setaram) with a universal TG-TD head was used for combined TGA and DTA. A 200-mg sample was heated in a Pt crucible from room temperature to 1030 °C using a 4 °C/min heating rate. Temperature, sample weight and differential weight were recorded simultaneously on a personal computer.

IR Spectroscopy

Diffuse reflectance IR spectra were obtained on a Bruker IFS 88 Fourier transform IR spectrometer equipped with a mercury–cadmium–telluride (MCT) detector and a diffuse reflectance accessory (Harrick Corporation). Seventy milligrams of sample was diluted in 370 mg of KBr and 200 scans were recorded at a resolution of 4 cm^{-1}.

EPR Measurements

The EPR spectra were obtained at 293 K with an X-Band Brüker ER 200 spectrometer using randomly oriented powders in air-dried and water-soaked conditions (Mosser et al. 1990). Dry samples were inserted into quartz tubes and samples that were soaked in water for 48 h were measured in a flat glass cell.

XPS Measurements

The XPS spectra were recorded on a CAMECA-RIBER NANOSCAN 50 apparatus equipped with an Al$K\alpha$ source and a MAC 2 analyzer that was set at 1 eV energy resolution. The clays were dispersed in distilled water by ultrasonic treatment. A drop of that dispersion was placed onto a disk of 2-cm refractory vitreous carbon, air-dried and analyzed by XPS spectroscopy. The measurements were carried out after photoreduction times of 15 min, 2 h and 4 h according to the procedure described by Mosser et al. (1992). Indeed, it was shown that photoreduction effects can differentiate structural Cu locations in clay minerals.

Auger parameters were determined as well. The Auger parameter is defined as the difference in binding energy between the photoelectron and Auger lines. As static charge corrections cancel, this difference can be determined accurately. Auger parameter is very sensitive to the chemical state of the analyzed element, higher values being indicative of higher oxidation states.

RESULTS

X-ray Diffraction

Powder XRD patterns of laponite (Figure 1) exhibit very broad 001 reflections regardless of the interlayer cation and heating temperature. The $d(001)$ values obtained from these spectra are very approximative, as they correspond to the higher-angle value of the broad shoulder observed. The data reported in Table 1 and

https://doi.org/10.1346/CCMN.1997.0450603 Published online by Cambridge University Press

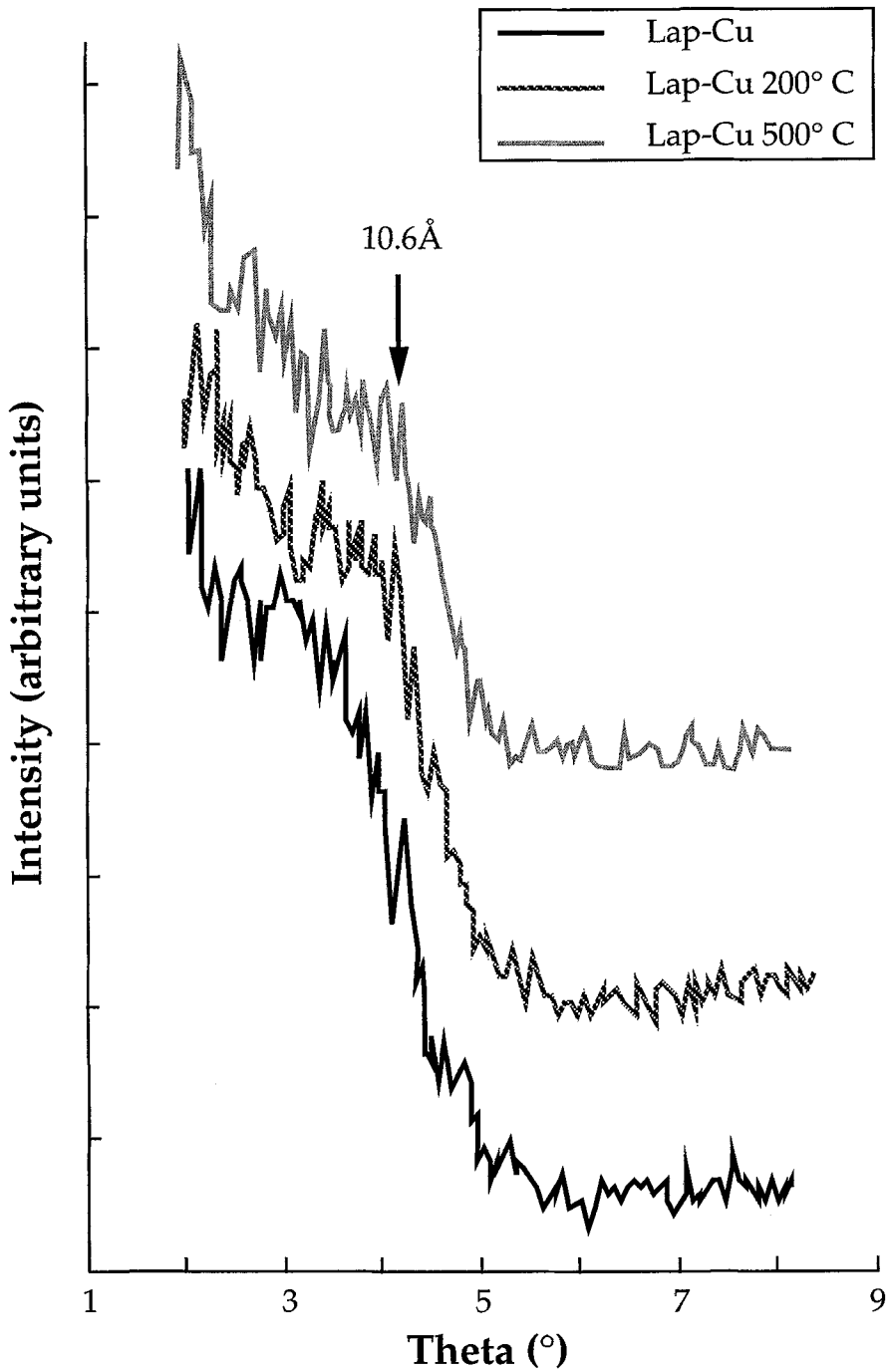

Figure 1. XRD patterns of Lap-Cu, Lap-Cu 200 °C and Lap-Cu 500 °C.

the spectra displayed in Figure 1 for Lap-Cu, Lap-Cu 200 °C and Lap-Cu 500 °C do not seem to suggest any significant change of the *d*-spacing with temperature.

For montmorillonite, the situation is quite different, as the 001 reflections are well defined. The starting Mont-Na presents a 001 reflection corresponding to a *d*-spacing of 12.6 Å under room atmosphere. It characterizes an interstratified system zero-layer hydrate–1-layer hydrate–2-layer hydrate (Cases et al. 1992; Bérend et al. 1995). After exchange with Cu the 001 reflection of Mont-Cu is located at 12.26 Å and is much sharper, which reveals the presence of a nearly homogeneous 1-layer hydrate state. The evolution of the *d*(001) with temperature is presented in Table 1.

https://doi.org/10.1346/CCMN.1997.0450603 Published online by Cambridge University Press

Table 2. CEC and interlayer composition of montmorillonite after Cu exchange and subsequent heat treatment.

Sample	Heating T (°C)	CEC	Cu	Ca	Mg	Na	Total
		(meq/100 g)					
Mont-Na	25	83	0	2.0	0.5	79	81.5
Mont-Cu	25	83	78.4	2.0	0.6	0.7	81.7
Mont-Cu	100	82	76.7	2.0	0.8	0.7	80.2
Mont-Cu	200	20	13.1	2.1	1.5	2.8	19.5
Mont-Cu	300	10	2.9	1.8	1.5	2.7	8.9
Mont-Cu	400	10	1.5	1.9	1.5	2.8	7.7
Mont-Cu	500	10	0.9	1.7	1.5	2.9	7.0

Table 3. CEC and interlayer composition of laponite after Cu exchange and subsequent heat treatment.

Sample	Heating T (°C)	CEC	Cu	Ca	Mg	Li	Na	Total
		(meq/100 g)						
Lap-Na	25	80	0	0.6	0.4	1.7	85.2	87.9
Lap-Cu	25	45	39.8	0.6	7.4	0.4	1.0	49.2
Lap-Cu	100	45	35.2	0.7	9.6	1.7	2.2	49.0
Lap-Cu	200	37	16.7	0.6	11.9	9.6	1.5	40.3
Lap-Cu	300	35	0.1	0.6	17.8	21.5	1.0	41.0
Lap-Cu	400	34	0	0.2	7.0	30.5	0.6	38.3
Lap-Cu	500	36	0	0.5	9.0	34.2	1.0	44.7

The d-spacing drops drastically to a value of 9.9 Å at 200 °C, revealing a quasi-complete dehydration of the interlayer cation. It then decreases regularly with increasing temperature. After heating at 500 °C, it is located at 9.5 Å.

CEC Measurements

The evolution of the CEC with Cu exchange and subsequent heat treatment at various temperatures is presented in Table 2 for montmorillonite and Table 3 for laponite. The composition of the interlayer determined from the analysis of the supernatant after exchange with cobaltihexamine is also presented.

The CEC of Mont-Cu remains the same as in the starting Mont-Na. Nearly all of the Na has been exchanged, as Cu represents 95% of the total milliequivalents. The CEC decreases drastically when the sample is heated to 200 °C (Mont-Cu 200 °C) as it is equal to 20 meq/100 g. For higher temperatures, the CEC remains constant at 10 meq/100 g. This behavior is consistent with a classical Hofmann–Klemen effect as if, upon heating, dehydrated Cu migrates toward the lacunae of the octahedral layer through the hexagonal cavity formed by the arrangement of the silica tetrahedra.

The behavior of laponite is quite different as, upon Cu exchange and freeze-drying, the CEC decreases from 80 meq/100 g (Lap-Na) to 45 meq/100 g (Lap-Cu) (Table 3). Heating at 100 °C has very little effect. When the sample is heated to 200 °C, the CEC de-

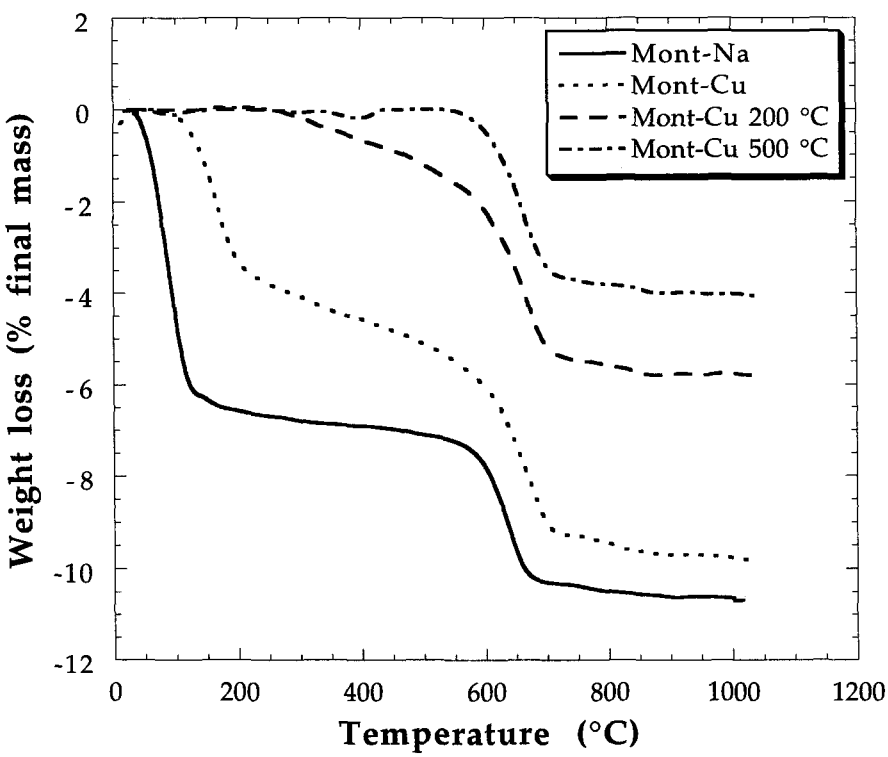

Figure 2. TGA of Mont-Na and of Mont-Cu preheated at 25, 200 and 500 °C.

https://doi.org/10.1346/CCMN.1997.0450603 Published online by Cambridge University Press

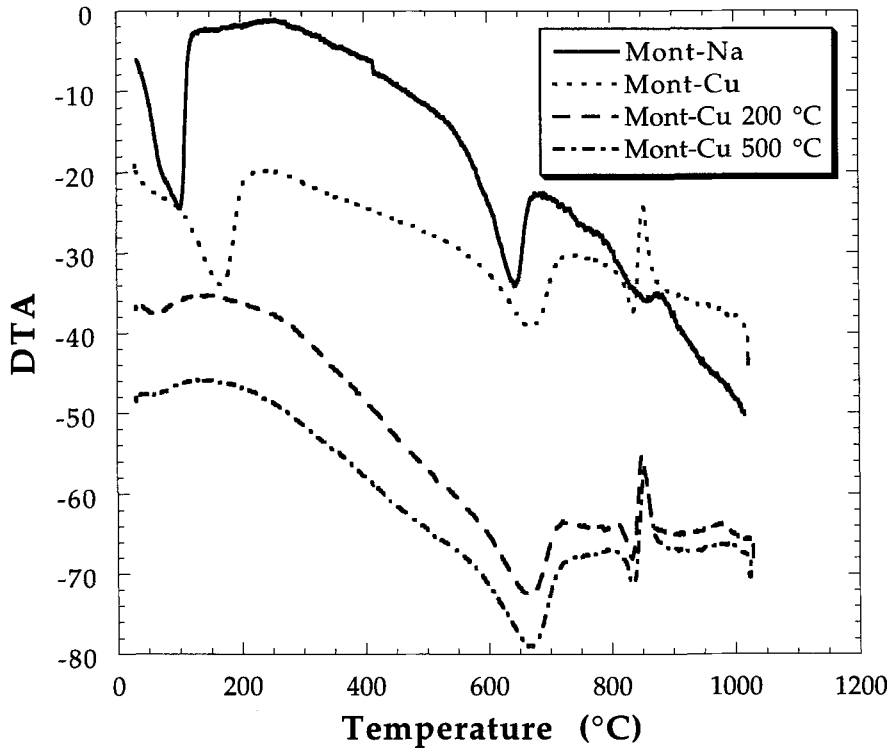

Figure 3. DTA of Mont-Na and of Mont-Cu preheated at 25, 200 and 500 °C.

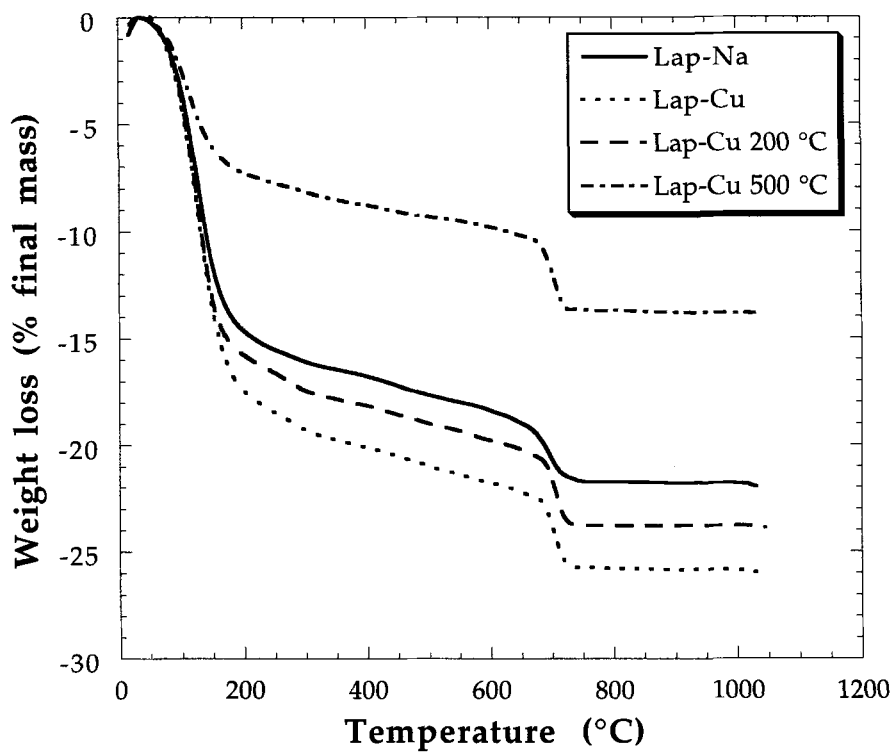

Figure 4. TGA of Lap-Na and of Lap-Cu preheated at 25, 200 and 500 °C.

https://doi.org/10.1346/CCMN.1997.0450603 Published online by Cambridge University Press

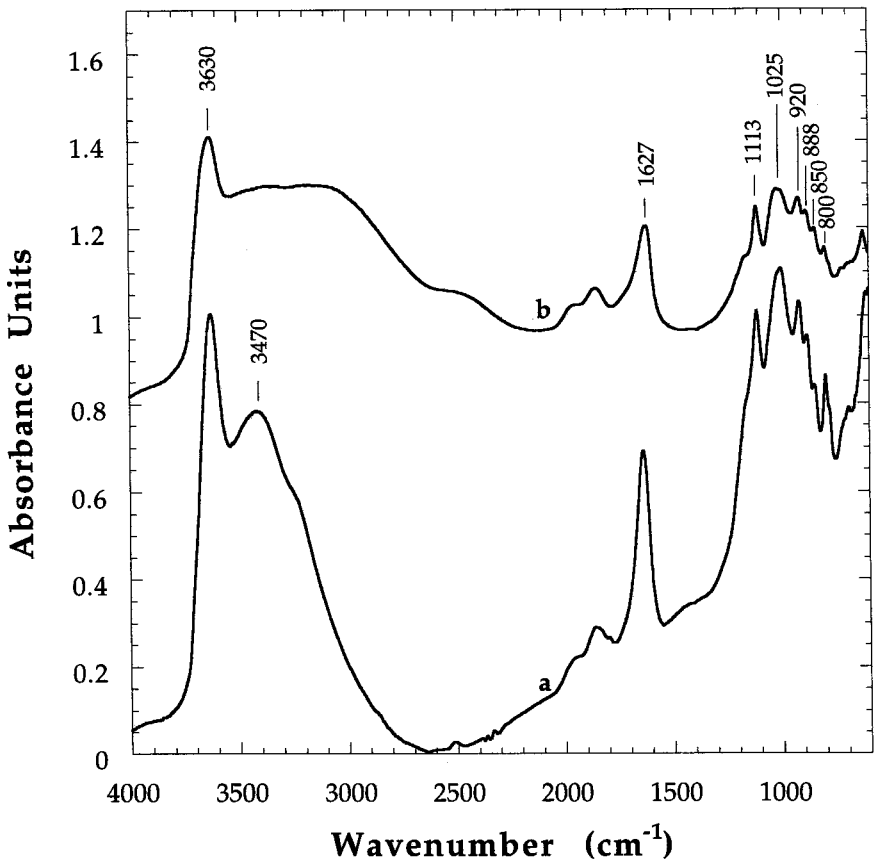

Figure 5. Diffuse reflectance IR spectra of a) Mont-Na, b) Mont-Cu.

creases to ≈35 meq/100 g, the amount of exchangeable Cu diminishes and Li appears in the interlayer. Above 200 °C, there is no more exchangeable Cu and the amount of Li increases while the CEC remains constant around 35 meq/100 g. As chemical analyses of Lap-Cu reveal the absence of Na and a high copper content (4.74%), the CEC decrease observed upon Cu exchange is likely due to the selective dissolution of the octahedral sheet with regard to the tetrahedral sheet upon exchange in the acidic (pH ≈ 4) copper sulfate solution. The presence of small amounts of Mg in the solution confirms this mechanism as it shows that some Mg from the octahedral sheet has been released from the clay layer. Furthermore, a similar behavior was observed by Kreit et al. (1982) in the case of a natural Na-hectorite stirred 3 times in 10^{-4} *N* salt solutions (Na, Li, Mg or Ca-chlorides) which exhibited a 40% CEC decrease. The high Cu content suggests that some surface-induced hydrolysis has occurred, resulting in nonexchangeable Cu species. This was also observed by McBride (1982) in his study of Cu-hectorite. The presence of nonexchangeable surface species is confirmed by the XRD patterns obtained at high temperature (400 and 500 °C), which exhibit very small amounts of copper oxides. These hydrolyzed Cu species are not present on montmorillonite, as evidenced by the studies of Stadler and Schindler (1993). They show that for pH ≤ 4, most of the Cu adsorbed by montmorillonite is exchanged $Cu(H_2O)_6^{2+}$.

Thermal Analysis

The TGA curves corresponding to Mont-Na, Mont-Cu, Mont-Cu 200 °C and Mont-Cu 500 °C are presented in Figure 2. The curve corresponding to Mont-Na exhibits a first weight loss between 25 and 100 °C, corresponding to the loss of physisorbed water and of the first water molecules bound to the sodium cation. Between 100 and 580 °C, the last water molecules surrounding the cation are eliminated and the dehydroxylation of the structure might start occurring. Around 600 °C, a sharp weight loss corresponds to the dehydroxylation of the structure. In the case of Mont-Cu, the weight loss corresponding to the first dehydration of the interlayer cation is shifted towards higher temperatures, revealing the stronger interaction between Cu and the water molecules. The weight loss between 200 and 580 °C is also more important. The dehydroxylation temperature is nearly unaffected by the nature of the interlayer cation. After heating at 200 °C, there is a weight loss corresponding to the elimination

https://doi.org/10.1346/CCMN.1997.0450603 Published online by Cambridge University Press

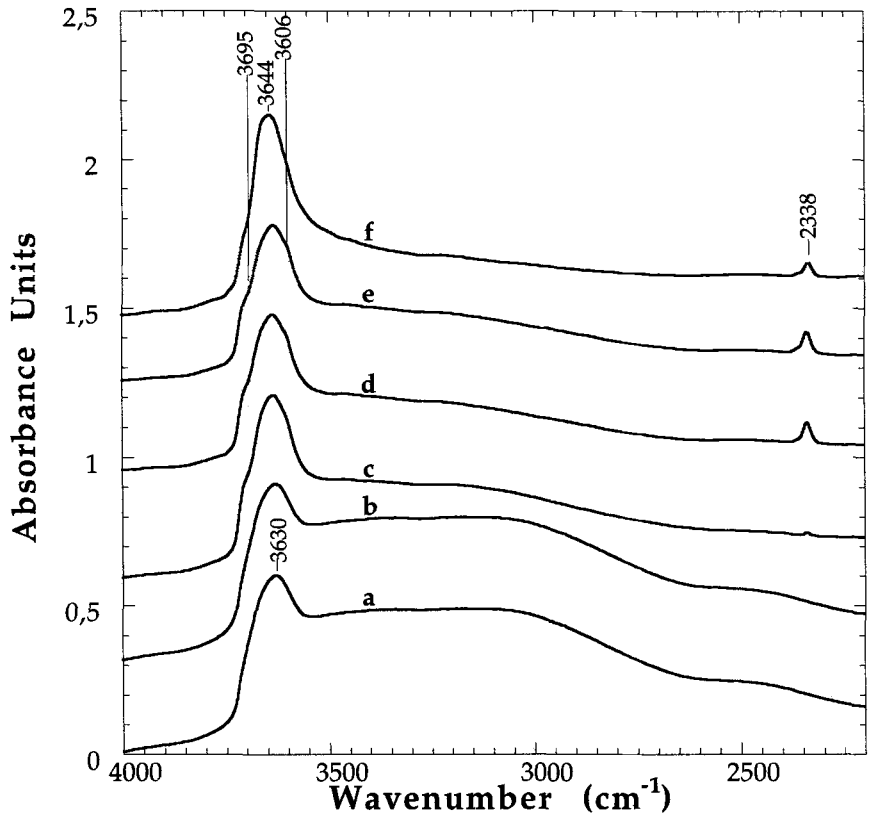

Figure 6. Diffuse reflectance IR spectra (range 4000–2200 cm^{-1}) of Mont-Cu heated at a) 25 °C, b) 100 °C, c) 200 °C, d) 300 °C, e) 400 °C f) 500 °C.

of the last water molecules bound to the cation which disappears after heating at 500 °C. In all cases, the dehydroxylation temperature is unchanged.

The DTA curves are presented in Figure 3. In the low-temperature range, the DTA reveal the same trends as the TGA measurements. The dehydration of Mont-Cu is shifted towards higher temperature with respect to the starting Mont-Na. The main dehydroxylation around 650 °C is unaffected by the Cu exchange. On the contrary, the pattern of the endothermic peak immediately followed by an exothermic peak indicating recrystallization around 850 °C is modified upon Cu exchange as the phenomenon is much sharper in the case of Mont-Cu. This change in the recrystallization reaction reveals a different composition of the octahedral layer, after Cu exchange and heating. The preheating does not have any effect as Mont-Cu, Mont-Cu 200 °C and Mont-Cu 500 °C exhibit exactly the same pattern in this range.

The TGA curves obtained for Lap-Na, Lap-Cu, Lap-Cu 200 °C and Lap-Cu 500 °C are presented in Figure 4. The total amount of water lost is always higher than in the case of montmorillonite. This is likely due to freeze-drying. Indeed, laponite particles are much smaller than montmorillonites and can form a network enclosing various pores upon freeze-drying. The behavior is also different from what was observed in the case of montmorillonite. Indeed, the dehydration temperature is not affected by the Cu exchange, as roughly the same amount of water is lost by Lap-Na, Lap-Cu and Lap-Cu 200 °C. Only after preheating at 500 °C, the amount of hydration water is diminished. The presence of hydration water reveals the same trends as the CEC measurements, that is, the interlayer space is still partially available. The dehydroxylation temperature seems unaffected. The corresponding DTA curves (not presented) exhibit the same trends as in the case of montmorillonite, that is, modifications in the high-temperature range (>650 °C) revealing changes in the composition of the octahedral sheet.

IR Spectroscopy

The IR spectra corresponding to Mont-Na and Mont-Cu are presented in Figure 5. The main difference lies in the OH stretching vibrations corresponding to the hydration shell of the cations that are shifted toward lower wave numbers when Cu is the interlayer cation. The evolution of the IR spectra of Mont-Cu with heating is presented in Figure 6 for the range 4000–2200 and Figure 7 for the range 2200–600 cm^{-1}.

https://doi.org/10.1346/CCMN.1997.0450603 Published online by Cambridge University Press

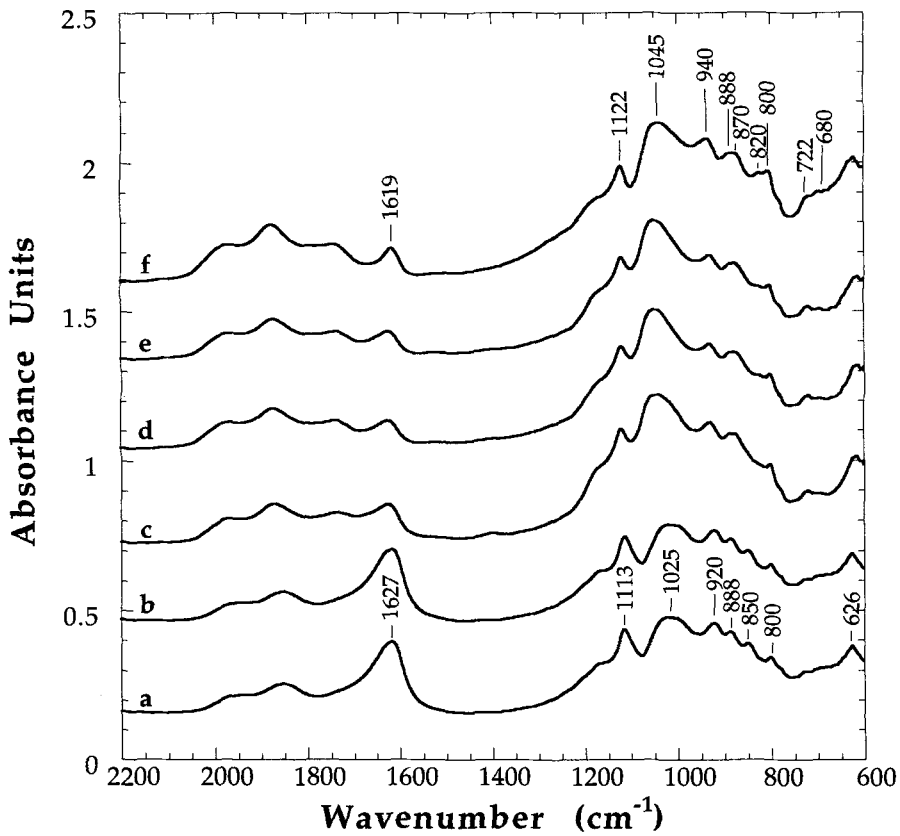

Figure 7. Diffuse reflectance IR spectra (range 2200–600 cm^{-1}) of Mont-Cu heated at a) 25 °C, b) 100 °C, c) 200 °C, d) 300 °C, e) 400 °C, f) 500 °C.

In the range 4000–2200 cm^{-1} (Figure 6), 5 main features can be noticed, for temperatures higher than 200 °C: 1) The bands corresponding to the stretching of OH groups belonging to the hydration shell of the interlayer cation nearly totally disappear, which confirms the TGA analyses. 2) The band at 3630 cm^{-1} corresponding to the stretching vibration of hydroxyl groups surrounded by 2 Al (Farmer and Russell 1971; Poinsignon 1978) shifts towards higher wave numbers at 3644 cm^{-1}. 3) A shoulder appears on the high-frequency side at 3695 cm^{-1}. 4) A shoulder at 3606 cm^{-1} appears. This position seems to be related to the presence of Fe(III) (Farmer 1971; Poinsignon 1978). 5) A band at 2338 cm^{-1}, which can be assigned to liquid carbon dioxide, appears.

In the range 2200–600 cm^{-1} (Figure 7), many changes of the spectra can be noticed, for temperatures higher than 200 °C. The deformation of OH groups belonging to the hydration shell of the interlayer cation around 1630 cm^{-1} are strongly diminished and shifted towards lower wave number at 1619 cm^{-1}. The bands corresponding to the deformation of OH groups surrounded by Fe(III)-Al (888 cm^{-1}) and Mg-Fe(III) (800 cm^{-1}) do not seem to be affected. On the contrary, the bands corresponding to the deformation of OH groups surrounded by Al-Al (920 cm^{-1}) and Mg-Al (850 cm^{-1}), are shifted towards higher wave numbers at 940 and 870 cm^{-1}, respectively. New bands appear at 820, 722 and around 680 cm^{-1}. Concomitantly the bands corresponding to the Si-O-Si stretching vibrations at 1113 and 1025 cm^{-1} are shifted towards higher wave numbers at 1122 and 1045 cm^{-1}. The same shifts can be noticed on the combination bands in the 1900–1700 cm^{-1} region.

All these results suggest the presence of Cu(II) atoms in the octahedral layer of Mont-Cu as soon as the temperature is higher than 200 °C. This can be noted by the band at 3644 cm^{-1}, which was already observed in synthetic cupriferous kaolinites (Petit 1990) and was assigned to Cu-OH stretching vibrations. For this study, this band could also result from a shift of the 3630 cm^{-1} Al_2OH band due to a more trioctahedral character. The band around 820 and 720 cm^{-1} could correspond to Cu-O-Si stretching vibrations, as observed in chrysocolle (Petit 1990); whereas the band around 680 cm^{-1} could be assigned to Cu-OH deformation vibrations. All the bands corresponding to OH surrounded by Fe(III) atoms are not affected by the presence of Cu, which suggests that Cu in the octahedral sheet is not located close to Fe(III) atoms. On

https://doi.org/10.1346/CCMN.1997.0450603 Published online by Cambridge University Press

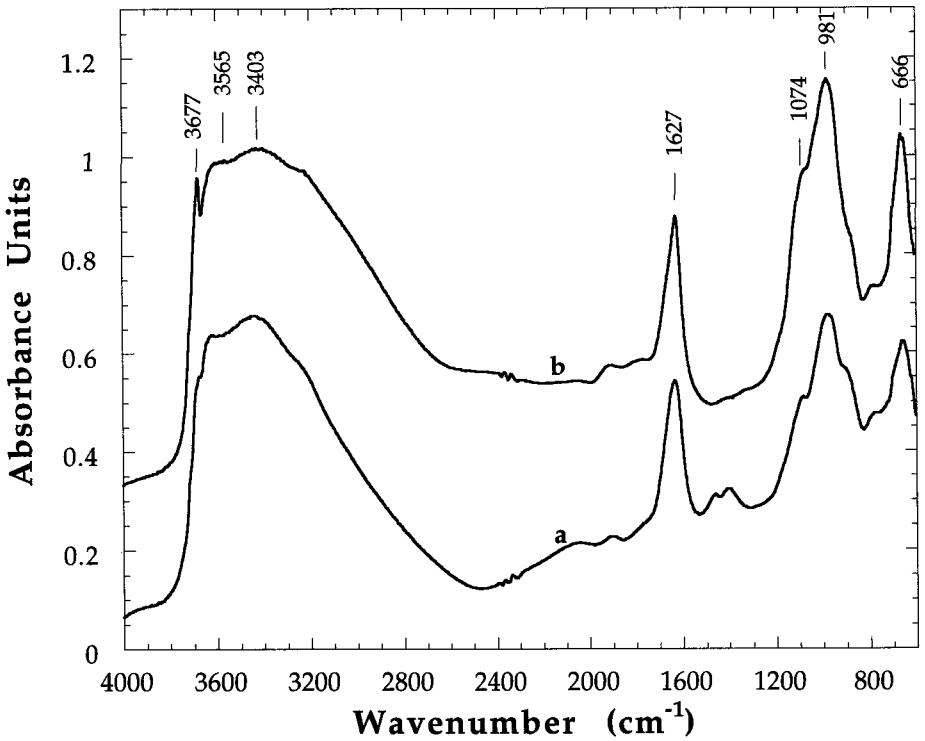

Figure 8. Diffuse reflectance IR spectra of a) Lap-Na, b) Lap-Cu.

the contrary, Al_2OH and Al-Mg OH vibrations are strongly affected by the presence of Cu.

The IR spectra corresponding to Lap-Na and Lap-Cu are presented in Figure 8. There are very little differences between the 2 spectra except in the OH stretching vibration range, where the band at 3677 cm^{-1} corresponding to Mg_3-OH is better defined in the case of Lap-Cu.

The evolution of the IR spectra of Lap-Cu with heating is presented in Figure 9. As revealed by CEC measurements and TGA data, bands corresponding to the stretching and deformation of OH groups of hydration water are always present. The main feature of this spectra is the appearance for temperatures higher than 200 °C of a band at 3650 cm^{-1}, which is likely to correspond to Cu-Mg_2-OH or Cu-Mg-Li-OH vibrations revealing the presence of Cu atoms in the octahedral layer. Three features can be noted on these spectra: 1) The bands corresponding to Si-O-Si are affected by Cu exchange and subsequent heating. The band at 981 cm^{-1} shifts towards higher wave numbers at 996 cm^{-1}. 2) A combination band at 1809 cm^{-1} appears for temperatures higher than 200 °C. 3) A very small band located around 830 cm^{-1} appears for heating temperatures of 400 and 500 °C.

EPR

The EPR spectra of Mont-Cu heated at different temperatures are presented in Figure 10. Figure 10A corresponds to the dry samples and Figure 10B to the wet state (water soaked for 48 h). The signals around g = 4.4 to 4.5 correspond to octahedral Fe(III) atoms and those around g = 2 to Cu(II) atoms.

At all temperatures, the EPR spectra of the air-dried samples (Figure 10A) present an anisotropic signal with g = 2.05, revealing that Cu is in a restricted environment. When compared with Fe(III) octahedral signal at g = 4.53, it appears that the Cu signal, at 2.05, presents a progressive loss of intensity from 25 to 500 °C, which can be assigned to lattice relaxation effects (McBride and Mortland 1974; Heller-Kallai and Mosser 1995).

From room temperature to 500 °C, the EPR signals of the 48-h water-soaked samples (Figure 10B) exhibit an evolution from isotropic (T = 25 °C, 100 °C, g = 2.15) to anisotropic (T = 300 °C to 500 °C, g = 2.05). At 200 °C both signals are present. The evolution of these EPR spectra show a transition between Cu in position reachable by water (g = 2.15) to positions that water molecules cannot reach (g = 2.05). At room temperature, Cu is located in the interlayer region and upon hydration will form $Cu(H_2O)_6^{2+}$ species, which tumble rapidly at the surface. At 300 °C, the signal remains nearly isotropic, but is located at g = 2.05. Above 300 °C, the signal becomes anisotropic as in the case of air-dried samples. This shows a change in the symmetry of Cu and of its ligand sphere. It can be interpreted as the migration of Cu from the bottom of

https://doi.org/10.1346/CCMN.1997.0450603 Published online by Cambridge University Press

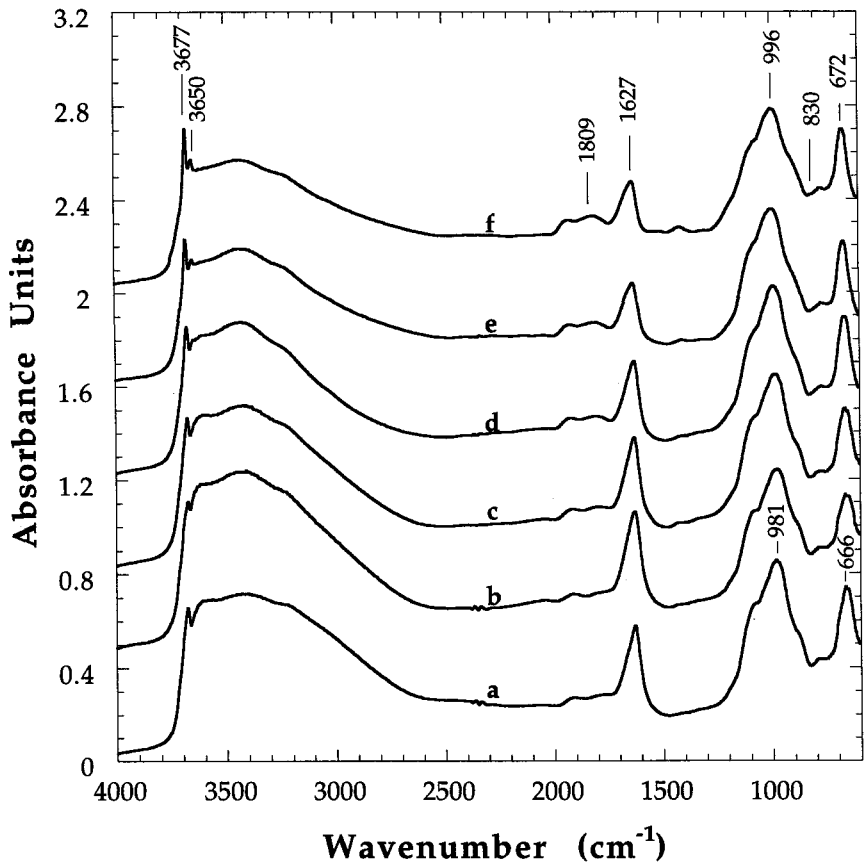

Figure 9. Diffuse reflectance IR spectra of Lap-Cu heated at a) 25 °C, b) 100 °C, c) 200 °C, d) 300 °C, e) 400 °C, f) 500 °C.

the hexagonal cavity into the vacant octahedral sites of the montmorillonite structure.

The EPR spectra of Lap-Cu heated at different temperatures are presented in Figure 11A for the dry samples and in Figure 11B for the wet ones. No Fe(III) is present in the structure and only the Cu(II) signal around $g = 2$ can be observed.

With increasing temperature, the EPR spectra of the air-dried samples (Figure 11A) exhibit an evolution from anisotropic (T = 25 °C, 100 °C, $g = 2.05$ with a perpendicular and a parallel component) to isotropic (T = 300 °C to 500 °C, $g = 2.05$). It shows a change in the location of Cu, the isotropic signal resulting from magnetic interactions as Cu come close to each other.

The EPR spectra of the 48-h water-soaked samples (Figure 11B) change with increasing temperature. At 25 °C, the signal is mainly isotropic at $g = 2.15$ with a width of 118 G. Small shoulders at $g = 2.33$ and $g = 2.05$ can be observed. This reveals at least 2 positions for Cu. The most important one generates the isotropic peak at $g = 2.15$ and can be assigned to Cu in interlamellar position surrounded by water molecules. The second signal barely visible (shoulders at $g = 2.33$ and $g = 2.05$) corresponds to Cu in restricted position not influenced by surrounding water molecules. It can be tentatively assigned to the nonexchangeable Cu species suggested by the CEC and chemical analyses and observed by XRD. At 500 °C, an isotropic signal at $g = 2.05$ with a width of 430 G can still be observed. Cu is in positions where it cannot be reached by water ($g = 2.05$). The widening of the signal from 118 G at 25 °C to 430 G at 500 °C reveals a strong magnetic interaction due to Cu clustering. CEC measurements showed that, at this temperature, Li was the main component present in the interlayer space whereas there was no Cu in exchangeable position. This could mean that Li was in clustered octahedral positions in the starting synthetic laponite. At 200 °C, 2 signals at $g = 2.05$ and $g = 2.15$ can be observed. This corresponds to the beginning of the migration of Cu into the structure, at least near the OH position at the bottom of the hexagonal cavity.

XPS

Room temperature (25 °C), heated at 200 °C and at 500 °C Mont-Cu and Lap-Cu were studied by XPS spectroscopy.

https://doi.org/10.1346/CCMN.1997.0450603 Published online by Cambridge University Press

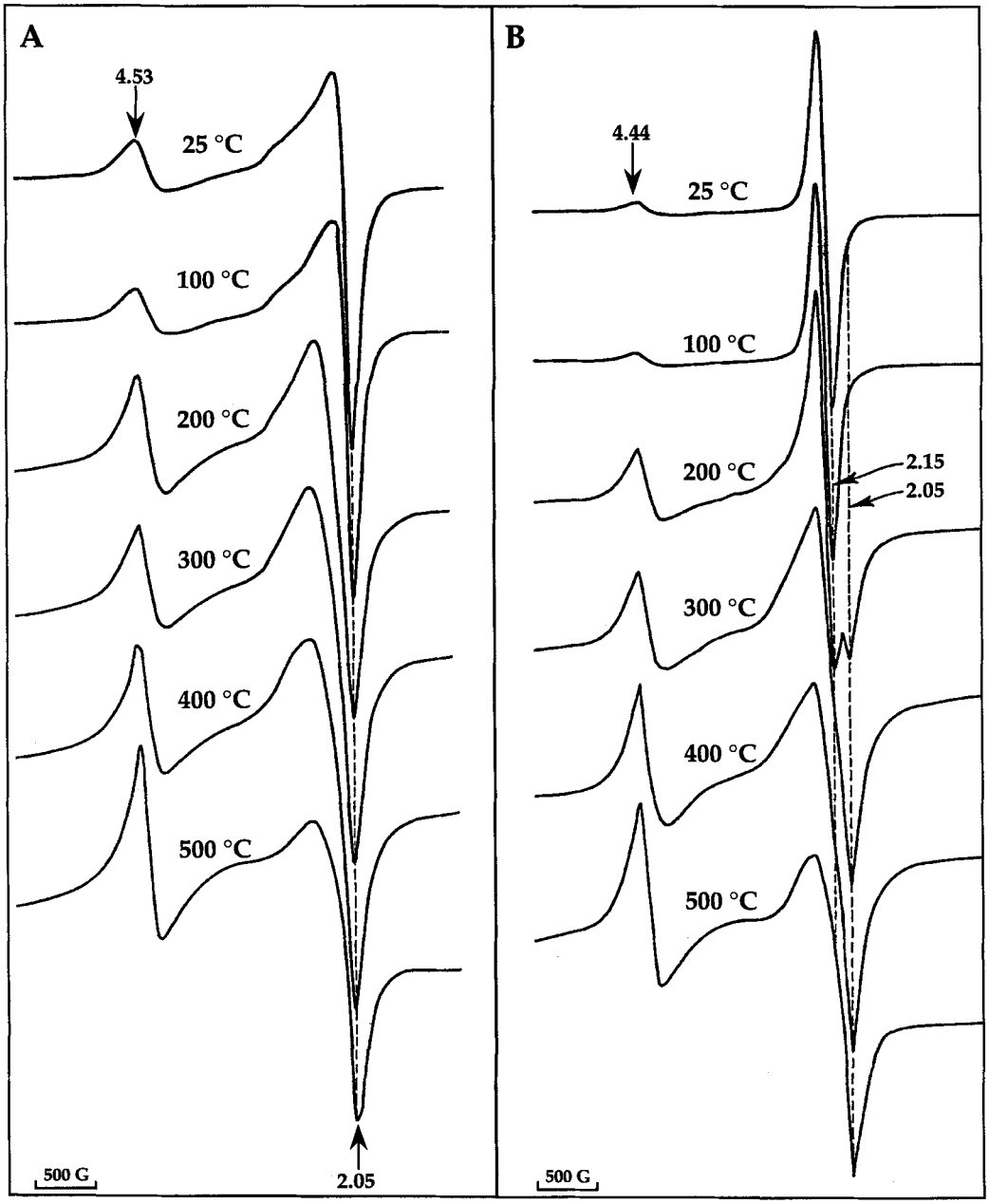

Figure 10. EPR spectra of Mont-Cu heated at various temperatures. A) dry sample, B) wet sample.

The relative intensity of shake-up satellites is useful in identifying the chemical state of Cu (Wagner et al. 1978). With O ligands, copper presents well-defined shake-up satellites when in Cu(II) state and none when in reduced (Cu(I)) state. Table 4 presents, for 3 photoreduction times (15 min, 2 h and 4 h), the relative intensities of shake-up satellites versus Cu 2p 3/2 (in arbitrary units) for Mont-Cu and Lap-Cu at room temperature and heated at 200 °C and 500 °C.

At room temperature, Lap-Cu presents low relative shake-up intensities for the 3 photoreduction times (0.19–15 min, 0.14–2 h and 0.15–4 h) which are in good accordance with Cu in interlamellar position. At 200 °C, a higher relative shake-up intensity (0.32) is observed after 15 min photoreduction. This value decreases strongly for photoreduction times of 2 h (0.13) and 4 h (0.12). At 500 °C, high relative shake-up intensities are observed for the 3 photoreduction times (0.50, 0.40 and 0.43). The absence of photoreduction effect reveals that Cu reacts as if in octahedral position. The migration of Cu from the interlamellar region towards octahedral positions starts occuring around

https://doi.org/10.1346/CCMN.1997.0450603 Published online by Cambridge University Press

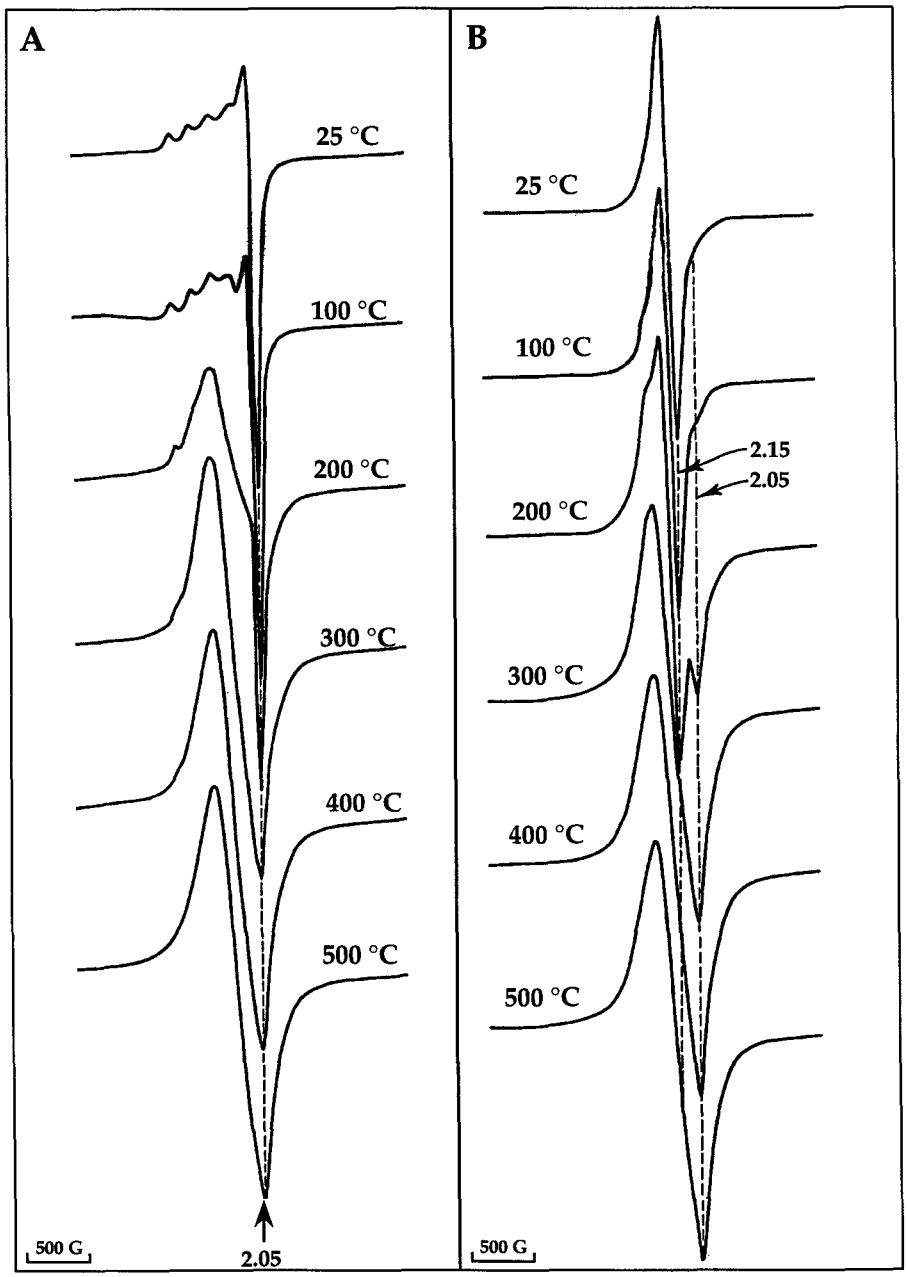

Figure 11. EPR spectra of Lap-Cu heated at various temperatures. A) dry sample, B) wet sample.

Table 4. Shake-up intensity versus Cu 2p 3/2 peak intensity in arbitrary units.

	Photoreduction time		
	15 min	2 h	4 h
Lap-Cu 25 °C	0.19	0.14	0.15
Lap-Cu 200 °C	0.32	0.13	0.12
Lap-Cu 500 °C	0.50	0.40	0.43
Mont-Cu 25 °C	0.20	0.12	0.12
Mont-Cu 200 °C	0.32	0.36	0.36
Mont-Cu 500 °C	0.50	0.42	0.56

200 °C. As Cu remains sensitive to photoreduction, it is likely located near the OH position at the bottom of the hexagonal cavity.

At room temperature, Mont-Cu exhibits low relative shake-up intensities for the 3 photoreduction times (0.20–15 min, 0.12–2 h, 0.12–4 h) revealing, as in the case of Lap-Cu, the presence of Cu in the interlayer region. At 200 °C, higher relative intensities (0.32, 0.36 and 0.36) are observed for the 3 photoreduction times, which is also the case at 500 °C with even higher values (0.50, 0.42, 0.56). The absence of any pho-

https://doi.org/10.1346/CCMN.1997.0450603 Published online by Cambridge University Press

Table 5. Auger parameters plus photon energy (1486.6 eV) of Lap-Cu and Mont-Cu at room temperature, heated at 200 °C and at 500 °C.

	25 °C	200 °C	500 °C
Lap-Cu	1847.3	1847.4	1850.0
Mont-Cu	1845.8	1847.6	1847.2

toreduction effect shows that, at both temperatures, Cu is firmly bonded to structural ligands. The lower values obtained at 200 °C can be interpreted as revealing a strong OH bond (stronger than in the case of Lap-Cu) whereas the results obtained at 500 °C suggest an octahedral position.

Auger parameters were measured for Mont-Cu and Lap-Cu at room temperature, 200 and 500 °C (Table 5). The measurements were performed after 5 h exposure to the X-ray photoelectrons for laponite and after 10 h for montmorillonite. Therefore, the values obtained for the 2 minerals cannot be exploited directly and only relative variations can be compared.

For Lap-Cu, the Auger parameters are the same (1847.3 and 1847.4) for the room temperature and 200 °C samples and higher (1850.0) for the 500 °C sample. These values reveal an octahedral position for Cu at 500 °C and a less-bonded situation, probably closer to the interlamellar region, for Cu at room temperature and 200 °C.

For Mont-Cu, the Auger parameters are the same (1847.6 and 1847.2) for the 200 °C and 500 °C samples, and lower (1845.8) for the room temperature sample. The lower value is coherent with an interlamellar position, whereas at higher temperature, Cu becomes more firmly bonded to structural ligands. This occurs at lower temperatures than for Lap-Cu.

DISCUSSION

The case of Cu-exchanged montmorillonite does not deserve much discussion, as its behavior upon heating appears rather classical. All the employed techniques show that Cu is located mainly in the interlayer space for temperatures ≤200 °C. Its hydration shell diminishes with temperature. For temperatures >200 °C, Cu migrates into the octahedral lacunae, where they saturate the charge of the sheet. The remaining CEC is very small and is likely due mainly to charged sites on the edge of the montmorillonite sheets and to the few tetrahedral substitutions present in natural Wyoming montmorillonite. Two structural facts can, however, be derived from the infrared spectra: 1) all the bands corresponding to hydroxyl groups surrounded by Fe are not affected by Cu exchange; 2) the presence of a band around 690 cm^{-1} observed in chrysocolla corresponding to δ Cu_x-OH vibration suggests the presence of neighboring Cu-Cu in the octahedral sheet (Petit et al. 1995). This can also be observed on the EPR spectra, which exhibit a widening of the signal. This could reveal a certain amount of clustering of Cu atoms in trioctahedral domains. This type of behavior was also observed by extended X-ray absorption fine structure (EXAFS) in the case of heated Ni-exchanged montmorillonite (Besson et al. 1990).

In the case of Lap-Cu, the phenomena involved upon Cu exchange and subsequent heating appear more complicated. Cu exchange first provokes an hydrolysis of the starting Lap-Na, resulting in a loss of approximately 40% of the CEC. At 200 °C, the CEC measurements reveal that, per 100 g of clay, out of the starting 17.6 mmol of exchangeable Cu (at 100 °C), only 8.3 remain exchangeable. The 9.3 lost are "replaced" by 7.9 mmol of Li and 1.2 mmol of Mg, resulting in a CEC loss of 8 meq/100 g. The IR-barely visible band at 3650 cm^{-1} (Figure 9), XPS and EPR measurements reveal that nonexchangeable Cu is not located in structural position only, at this temperature. It seems that it could be partially sitting at the bottom of the hexagonal cavity. At 300 °C, the remaining 8.3 mmol of exchangeable Cu are migrating from the interlayer and are "replaced" by 3 mmol of Mg and 12 mmol of Li, resulting in no further CEC decrease. In that case, a band at 3650 cm^{-1} starts being more important on the IR spectra (Figure 9), whereas EPR results reveal that Cu atoms cannot be reached by water molecules (Figure 11b). Therefore, Cu atoms are mainly located in structural positions. This is even more obvious after heating at 400 or 500 °C. At 400 °C, another phenomenon is suggested from the CEC experiments. The composition of the interlayer space changes as the amount of Mg decreases, whereas the amount of Li increases. It therefore seems that Mg ions, as Cu ions, can remigrate into the structure to replace structural Li ions. In both cases, Cu between 200 and 300 °C or Mg between 300 and 400 °C, 1 divalent ion is replaced by 2 monovalent ions, which does not affect the overall charge of the layer.

All these results show that, for a trioctahedral clay mineral such as laponite, structural replacements in the octahedral layer can occur at relatively low temperatures (300 to 500 °C). These transformations mainly affect the substituting atom, such as Li, but seem to also affect the main component of the octahedral sheet, Mg. The substituting atom, whether it is Cu or Mg, likely accesses the octahedral sites through the hexagonal cavity formed by the arrangement of silica tetrahedra in the tetrahedral layer. The fact that both Mg and Cu exhibit the same behavior suggests that many other divalent cations could be accommodated in the octahedral layer, resulting in very variable compositions. It would certainly be interesting to study the location of the new divalent cations of the octahedral layer using local probes such as EXAFS to see whether there is a tendency to clustering as suggested by EPR.

ACKNOWLEDGMENTS

The authors wish to thank E. Bouquet for performing the CEC measurements.

REFERENCES

Alvero R, Alba MD, Castro MA, Trillo JM. 1994. Reversible migration of lithium in montmorillonites. J Phys Chem 98: 7848–7853.

Bérend I, Cases JM, François M, Uriot JP, Michot L, Masion A, Thomas F. 1995. Mechanism of adsorption–desorption of water vapor by homoionic montmorillonite: 2. The Li^+, Na^+, K^+, Rb^+ and Cs^+ exchanged forms. Clays Clay Miner 43:324–336.

Besson G, Decarreau A, Manceau A, Sanz J, Suquet H. 1990. Organisation interne du feuillet. In: Decarreau A, editor. Matériaux argileux, structure, propriétés, applications. SFMC editions. p 1–162.

Brindley GW, Lemaitre J. 1987. Thermal oxidation and reduction reactions of clay minerals. In: Newman ACD, editor. Chemistry of clays and clay minerals. Mineral Soc Monograph 6. p 319–370.

Calvet R, Prost R. 1971. Cation migration into empty octahedral sites and surface properties of clays. Clays Clay Miner 19:175–186.

Cases JM, Bérend I, Besson G, François M, Uriot JP, Thomas F, Poirier JE. 1992. Mechanism of adsorption–desorption of water vapor by homoionic montmorillonite: 1. The sodium exchanged form. Langmuir 8:2730–2739.

Cases JM, Delon JF, François M, Mercier R. 1981. Organisation de l'eau dans les milieux poreux ou concentrés en solides. [Compte-rendu de fin d'étude d'une recherche financée par la Délégation Générale à la Recherche Scientifique et Technique]. Nancy, France: INPL. 151 p.

Farmer VC, Russell JD. 1971. Interlamellar complexes in layer silicates. The structure of water in lamellar ionic solutions. Trans Faraday Soc 67:2737–2749.

Greene-Kelly R. 1953. Irreversible dehydration in montmorillonite. Clay Miner Bull 2:52–56.

Greene-Kelly R. 1955. Dehydration of the montmorillonite minerals. Mineral Mag 30:604–615.

Heller-Kallai L, Mosser C. 1995. Migration of Cu ions in Cu montmorillonite heated with and without alkali halides. Clays Clay Miner 43:738–743.

Hofmann U, Klemen R. 1950. Verlust der Austauschfähigkeit von Lithium Ionen an Bentonit durch Erhitzung. T Anorg Chemie 262:95–99.

Kreit JF, Shainberg I, Herbillon AJ. 1982. Hydrolysis and decomposition of hectorite in dilute salt solutions. Clays Clay Miner 30:223–231.

McBride MB. 1982. Hydrolysis and dehydration reactions of exchangeable Cu^{2+} on hectorite. Clays Clay Miner 30:200–206.

McBride MB, Mortland MM. 1974. Copper(II) interactions with montmorillonite: Evidence from physical methods. Soil Sci Soc Am Proc 38:408–414.

Mosser C, Mestdagh M, Decarreau A, Herbillon AJ. 1990. Spectroscopic (ESR, EXAFS) evidence of Cu for (Al-Mg) substitution in octahedral sheets of smectites. Clay Miner 25:271–282.

Mosser C, Mosser A, Romeo M, Petit S, Decarreau A. 1992. Natural and synthetic copper phyllosilicates studied by XPS. Clays Clay Miner 40:593–599.

Petit S. 1990. Etude cristallochimique de kaolinites ferrifères et cuprifères de synthèse (150–250 °C) [Thèse de Doctorat]. Poitiers, France: Univ de Poitiers. 237 p.

Petit S, Decarreau A, Mosser C, Ehret G, Grauby O. 1995. Hydrothermal synthesis (250 °C) of copper-substituted kaolinites. Clays Clay Miner 43:482–494.

Poinsignon C. 1978. Etude de l'eau d'hydratation des cations compensateurs de la montmorillonite [Thèse Docteur es Sciences]. Nancy, France: INPL. 242 p.

Rémy JC, Orsini L. 1976. Utilisation du chlorure de cobaltihexamine pour la détermination simultanée de la capacité d'échange et des bases échangeables dans les sols. Sciences du Sol 4:269–275.

Stadler M, Schindler PW. 1993. Modeling of H^+ and Cu^{2+} adsorption on calcium-montmorillonite. Clays Clay Miner 41:288–296.

Wagner CD, Riggs WM, Davis LE, Moulder JF, Muilenberg GE. 1978. Handbook of X-ray photoelectron spectroscopy. Muillenberg GE, editor. Minnesota: Perkin-Elmer Corporation, Physical Electronics Division. 190 p.

(Received 22 February 1996; accepted 25 November 1996; Ms. 2792)